Journal of Membrane Science and Research 7 (2021) 273-279

Journal of Membrane Science & Research

journal homepage: www.msrjournal.com

Research Paper

Factors Affecting Hydroxide Ion Concentrations in Bipolar Membranes

Yingying Chen, James C. Baygents, Dominic Gervasio, James Farrell *

Department of Chemical and Environmental Engineering, University of Arizona, Tucson, AZ 85721, USA

Article info

Received 2020-12-22
Revised 2021-01-24
Accepted 2021-01-26
Available online 2021-01-26

Keywords

Bipolar membrane electrodialysis
Electrolyte
Nucleophilic attack
Nernst-Plank equations

Highlights

- Membrane hydroxide concentrations depend strongly on current density.
- High concentrations of electrolyte anions decrease membrane hydroxide levels.
- Membrane hydroxide concentrations can reach 3.7 M when producing 1 M NaOH.
- Increasing anion layer thickness increases membrane hydroxide concentrations.

Graphical abstract

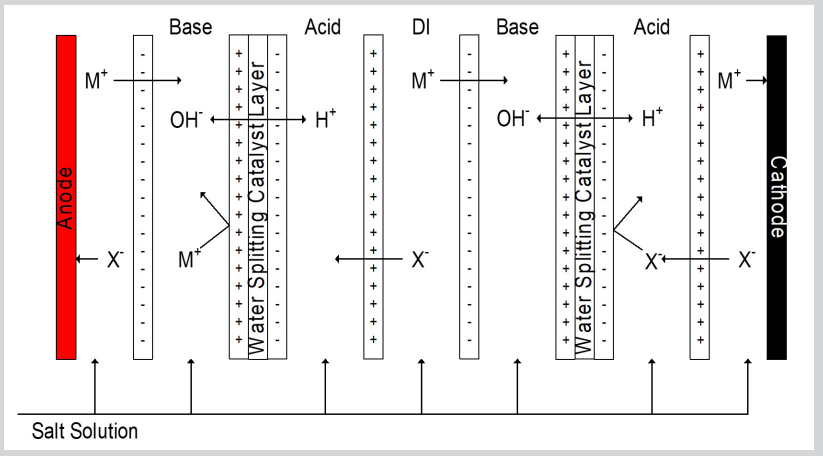

Abstract

The useful lifetime of bipolar ion exchange membranes is often limited by nucleophilic attack by hydroxide ions on the ionic groups and polymer backbone in the anion exchange layers (AELs). This is especially problematic in water treatment applications for making acid and base from salt solutions. This research investigated the effect of bulk electrolyte composition, current density, membrane thickness, ion exchange capacity, and bulk solution pH value on hydroxide ion concentrations inside the AELs of a bipolar membrane. One-dimensional Nernst-Plank equations were solved for the species Na^+, Cl^-, OH^- and H^+ within 20-100 µm thick anion and cation exchange layers with fixed charged densities ranging from 0.5-2.0 eq/L. In 1 M NaCl solutions at neutral pH values, hydroxide concentrations in the AEL reached as high as 2.2 M at a current density of 100 mA/cm². In 1 M NaOH solutions, hydroxide ion concentrations reached as high as 3.77 M. Hydroxide concentrations in the AEL were significantly affected by the ratio of Cl^- to hydroxide ions in the bulk electrolyte. Where hydroxide concentrations in the bulk electrolyte were an order of magnitude lower than chloride concentrations, membrane hydroxide concentrations were nearly proportional to the current density. Increases in ion exchange capacity and AEL thickness resulted in increased membrane hydroxide ion concentrations. Membrane concentrations of hydroxide ions can be minimized by operation at low current densities, with high background electrolyte concentrations using thin membranes with low ion exchange capacities and producing base concentrations less than 0.1 M.

1. Introduction

Bipolar membrane electrodialysis (BMED) is a process that is used in water treatment [1,2,3], food production [4,5,6], recovery of weak acids from fermentation broths [7,8], and in producing acid and base from brine solutions [9,10]. A bipolar membrane (BPM) consists of a strong acid cation exchange membrane laminated to a strong base anion exchange membrane. A weak base or weak acid catalyst is added to the interlayer between the two membranes to promote water dissociation into H^+ and OH^- ions. In BMED, a bipolar membrane is placed between monopolar cation and anion exchange membranes inside an electrochemical cell, as illustrated in Figure 1. An electrolyte solution is fed into the chambers between the membranes, and the electrodes are polarized as shown in Figure 1. The electric field results in electromigration of anions and cations out of the bipolar membrane and into the adjacent solution compartments of the cell. When the anions and cations are depleted from the interlayer region of the membrane, water splitting into H^+ and OH^- ions occurs in order to maintain the electrical current. Under most operating conditions, the potential drop across the transition region is approximately 1-2 V, and this change occurs over a distance of ~1 nm, resulting in electric fields on the order of 109 V/m [11]. Operation of the cell results in the production of a base solution on the anode side, and an acid solution on the cathode side, of the bipolar membrane. Charge neutrality is maintained by electromigration of cations into the base solution, and anions into the acid solution, from adjacent cell chambers. In commercial operations, a BMED stack may contain more than 100 of the unit cells illustrated in Figure 1.

Although polarization of the cell promotes electromigration of ions out of the bipolar membrane, ions in the bulk electrolyte solution may diffuse back

* Corresponding author:E-mail address: farrellj@email.arizona.edu (J. Farrell)

DOI: 10.22079/JMSR.2021.521613.1433

into the bipolar membrane as a result of concentration gradients between the bulk solution and the membrane. In the anion exchange layer (AEL) of the bipolar membrane there will be concentration gradients of both hydroxide ions and electrolyte anions. Charge neutrality in the membrane dictates that the bulk electrolyte anion concentration will affect the hydroxide concentration inside the anion exchange layer. Hydroxide ion migration through the anion exchange layer occurs via both electromigration and molecular diffusion. Factors affecting transport of hydroxide ions include: the electric field strength, membrane thickness, ion exchange capacity, bulk solution electrolyte concentration, and the hydroxide concentration gradient between the bipolar interface and the bulk solution.

Hydroxide ion concentrations inside the bipolar membrane will affect the rate of membrane degradation via nucleophilic substitution reactions [11,12]. However, the concentrations of OH^- and other ions cannot be experimentally measured, and will depend on the membrane properties and cell operating conditions. The goal of this research was to determine how the current density, membrane thickness, ion exchange capacity, bulk electrolyte ion concentrations, and bulk electrolyte pH value affect hydroxide ion concentrations in the anion exchange layers of a bipolar membrane. Towards that end, a mathematical model was developed to calculate the concentration distribution of Na^+, Cl^-, OH^- and H^+ ions inside the anion exchange layers of a bipolar membrane. This is the first research to model hydroxide ion concentrations in bipolar membranes.

2. Methods

2.1. Model geometry

A schematic diagram of the one-dimensional membrane model is shown in Figure 2. Properties of the membranes and BMED operating conditions were chosen to be similar to those of commercially available membranes under commonly used operating conditions [13]. The model consists of symmetric anion and cation exchange layers ranging from 20 to 100 µm in thickness, with fixed charged densities ranging from 0.5 to 2 eq/L and a dielectric constant (ϵ_r) of 20 [14]. The interface between the two membranes is centered at the origin, and the catalyst containing interlayer is not included in the model. The bulk solution was assumed to be uniformly mixed with no diffusion layer, and was defined to have a potential (ϕ_o) of zero. The bulk electrolyte was modeled as Na^+ and Cl^- with concentrations ranging from 0.0 to 1.0 M. Bulk solution OH^- and H^+ concentrations were varied from 0.0001 to 1.0 M, and current densities ranged from 0 to 100 mA/cm^2. These operating conditions are typical of real BMED applications [13]. The parameters and constants used in the modeling are listed in Table 1.

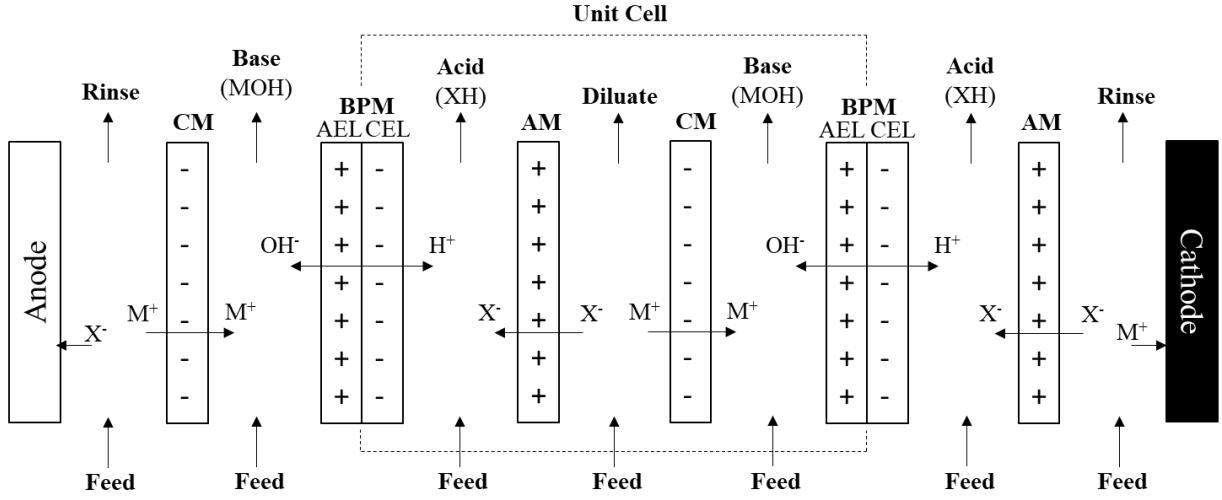

Fig. 1. Schematic drawing illustrating the production of acids (XH) and bases (MOH) from salt solutions (MX) using bipolar membrane electrodialysis. AEL – anion exchange layer; CEL – cation exchange layer; CM – monopolar cation exchange membrane; AM – monopolar anion exchange membrane.

2.1. Boundary Conditions

The boundary conditions at the left side of the AEL ($x=-\delta_A$) in contact with the bulk solution were modeled using Donnan equilibrium when no potential or current were applied to the system [15]. At equilibrium, there is no net flux (j) in the system, which can be expressed as:

$$j^k = -\frac{D^k dC^k}{dx} - \frac{D^k z^k F}{RT} C^k \frac{d\phi}{dx} = 0 \quad (1)$$

where: C is concentration, ϕ is potential and $k = Na^+, Cl^-, OH^- or\ H^+$.

Solving this equation yields:

$$C^k = B^k \exp\left(-\frac{z^k F}{RT}\phi\right), \text{where } B^k \text{ is a constant for each species } k. \quad (2)$$

Concentrations of each species in the bulk solution are known as C_o^k. The potential in the bulk solution, ϕ_o, is set to zero. Therefore, the constants B^k are solved as:

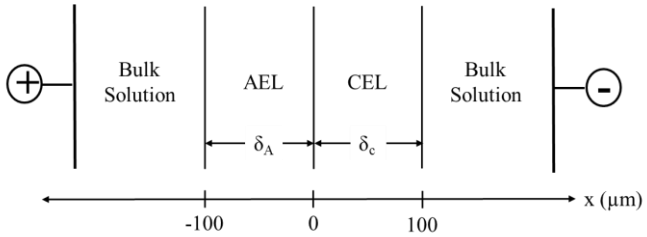

Fig. 2. Schematic diagram of the one-dimensional continuum model for the bipolar membrane with AEL and CEL thicknesses of 100 µm.

Table 1
Parameters used in this model.

Parameter	Value
Faraday's constant	F=96485 C/mol
Idea gas constant	R=8.314 J/mol K

Temperature	T=298.15 K
Vacuum permittivity	ϵ_o=8.854 x 10^{-12} F/m
Anion exchange layer charge density	ρ_{fix} = 0.5 to 2.0 eq/L
Cation exchange layer charge density	ρ_{fix} = -0.5 to -2.0 eq/L
Relative permittivity in membrane	ϵ_r=20
Valence	$z^{Na^+} = z^{H^+} = 1$ $z^{Cl^-} = z^{OH^-} = -1$
Diffusion coefficient [16]	$D^{H^+} = 5.94 \times 10^{-10}\ m^2/s$ $D^{OH^-} = 3.47 \times 10^{-10}\ m^2/s$ $D^{Na^+} = 7.98 \times 10^{-11}\ m^2/s$ $D^{Cl^-} = 2.39 \times 10^{-10}\ m^2/s$

$$B^k = C_0^k \exp\left(\frac{z^k F}{RT}\phi_0\right) \quad (3)$$

The ion concentrations in the AEL can then be expressed as:

$$C^k = C_0^k \exp\left(-\frac{z^k F}{RT}\phi\right) \quad (4)$$

For the concentration of species at the boundary at x = -δ_A, the potential at the boundary (ϕ_A) is put into equation (4) to yield:

$$C_A^k = C_0^k \exp\left(-\frac{z^k F}{RT}\phi_A\right) \quad (5)$$

For the boundary at x = -δ_A, electroneutrality leads to:

$$\begin{aligned} 0 &= \sum z^k C_A^k + \rho_{fix} \\ 0 &= (C_0^{Na^+} + C_0^{H^+})\exp\left(-\frac{F}{RT}\phi_A\right) - (C_0^{Cl^-} + C_0^{OH^-})\exp\left(\frac{F}{RT}\phi_A\right) + \rho_{fix} \\ 0 &= (C_0^{Na^+} + C_0^{H^+})\left[\exp\left(-\frac{F}{RT}\phi_A\right) - \exp\left(\frac{F}{RT}\phi_A\right)\right] + \rho_{fix} \end{aligned} \quad (6)$$

The potential at the AEL boundary at x = -δ_A was calculated by solving equation (6) to yield:

$$\phi_A = -\frac{RT}{F}\,asinh\left[-\frac{\rho_{fix}}{2(C_0^{Na^+} + C_0^{H^+})}\right] \quad (7)$$

A similar calculation process was applied for the boundary conditions at the CEL.

2.2. Governing Equations

The model solves four steady-state ordinary differential equations and one algebraic equation, given by the relation between the electric field and the electrostatic potential, material balance of electroneutrality in the AEL, and charge balance between the current and ion transport. The equations are listed below.

The first equation is the relation between the electric field (E) and the electrostatic potential (ϕ):

$$E = -\frac{d\phi}{dx} \quad (8)$$

The second equation results from electroneutrality throughout the AEL where the mobile ions are balanced by the fixed membrane charge density:

$$\sum z^k C^k + \rho_{fix} = 0 \quad (9)$$

Co-ion crossover in bipolar membranes is very low, and current efficiencies for water splitting in commercial membranes averages greater than 99% [17,18]. Thus, nearly all of the imposed current is carried by the transport of OH^- and H^+ ions. Expressing the current density in terms of only OH^- and H^+ ion transport leads to:

$$i = Z^{H^+} j^{H^+} F + Z^{OH^-} j^{OH^-} F \quad (10)$$

where flux $j^{H^+} = -D^{H^+}\left(\frac{dC^{H^+}}{dx} + \frac{z^{H^+}F}{RT}C^{H^+}\frac{d\phi}{dx}\right)$

and $j^{OH^-} = -D^{OH^-}\left(\frac{dC^{OH^-}}{dx} + \frac{z^{OH^-}F}{RT}C^{OH^-}\frac{d\phi}{dx}\right)$

following the Nernst Planck equation [19]. Also, the product of hydroxide and hydronium ion concentrations equals the dissociation constant of water:

$$K_W = C^{OH^-} \times C^{H^+} \quad (11)$$

For the last differential equation, the flux of each species is constant at steady state:

$$-\frac{dj^k}{dx} = \frac{dC^k}{dt} = 0 \quad (12)$$

Inserting the flux expressions into equation (12) yields:

$$0 = \sum z^k\left(\frac{dj^k}{dx}\right) = \sum z^k\left\{-D^k\left[\frac{d^2C^k}{dx^2} + \frac{z^kF}{RT}\frac{d}{dx}\left(C^k\frac{d\phi}{dx}\right)\right]\right\} \quad (13)$$

$$0 = -D^k\frac{d^2}{dx^2}\sum z^kC^k - \frac{D^kF}{RT}\frac{d}{dx}\left[\sum (z^k)^2C^k\frac{d\phi}{dx}\right]$$

The first term in equation (13) is zero, since $\rho_{fix}=\sum z^kC^k$ is a constant. Replacing $d\phi/dx$ with $-E$ in the second term of the equation, yields:

$$\sum (z^k)^2 C^k\frac{dE}{dx} + E\,\frac{d}{dx}\left[\sum (z^k)^2\,C^k\right] = 0 \quad (14)$$

which can be expressed as:

$$\frac{dE}{dx} = -E\,\frac{\frac{d}{dx}\sum (z^k)^2C^k}{\sum (z^k)^2C^k} \quad (15)$$

Four differential equations (8), (10), (12) and (15), and one algebraic equation (11) produces a differential-algebraic system of equations (DAE). A constant mass matrix of

$$M = \begin{bmatrix} 1 & 0 & 0 \\ 0 & 1 & 0 \\ 0 & 0 & 0 \end{bmatrix} \quad (16)$$

was used to represent the left hand side of the system of equations [20]. The DAE was solved in Matlab using the function ode15s [21]. A similar procedure was used to calculate the ionic distribution in the CEL.

Activity coefficients for the aqueous phase (γ_{aq}) were calculated using the Pitzer database in PHREEQC [22], which is an aqueous chemistry modeling program from the US Geological Survey. For the membrane phase, mean ion activity coefficients (γ_m) of 0.52 were used. This value was reported in Kamcev et al. [23] for a strong base anion exchange membrane with an exchange capacity of 1.44 eq/L, with a bulk solution NaCl concentration of 1 M. The model was run for bulk solution phases with NaCl and NaOH concentrations ranging from 0 to 1 M. Bulk solution concentrations of 1 M NaCl were selected to mimic feed solutions to a BMED stack, while 1 M NaOH bulk solutions were selected to mimic the final product solutions produced via BMED.

3. Results and discussion

3.1. Ion concentration profiles in AEL and CEL

Calculations at a current density of zero can be used to understand Donnan potential effects on the concentration profiles of ions in the bipolar membrane. Ion concentrations in the membrane phase (C^k) are related to those in the aqueous phase (C_{aq}^k) by:

$$C^k = \frac{\gamma_{aq}^k \cdot C_{aq}^k}{\gamma_m^k} \times \frac{1}{exp\left[\frac{z^k F(\phi - \phi_0)}{RT}\right]} \quad (17)$$

where γ_m^k and γ_{aq}^k are the activity coefficients for species k in the membrane and aqueous phases, respectively. For the membrane with an ion exchange capacity of 2 eq/L, the Donnan potential is 0.0208 V. Figure 3 shows the ion concentration profiles for a bulk solution consisting of 1 M NaCl + 0.1 M NaOH on the AEL side and 1 M NaCl + 0.1 M HCl on the CEL side. Activity coefficients for the aqueous phase species in these two solutions are shown in Table 2. The model results show the ion concentration profiles in the BPM at equilibrium with the bulk solution on each side. In this figure, x=0 represents the point of contact between the AEL and CEL, hereafter referred to as the bipolar interface. The bulk solution adjacent to the AEL is given by x<-100 µm and adjacent to the CEL is given by x>100 µm. Due to the Donnan potential and activity coefficient effects, the OH^- concentration in the AEL is 2.4 times higher, and the Cl^- concentration is 2.5 times higher, than those in the in bulk solution. In the CEL, H^+ and Na^+ concentrations are, respectively, 4.3 and 2.3 times greater than those in the bulk solution. The total mobile anion concentration in the AEL is 2.70 M, which exceeds the fixed charge concentration of 2.0 M. Mobile anion concentrations in excess of the fixed charge in the AEL are compensated by Na^+ and H^+ ions.

3.2. Bulk electrolyte effects

The effect of current density on hydroxide ion concentrations in the AEL are shown in Figures 4a,b for bulk solutions of 1 M NaCl and 1 M NaOH. Activity coefficients for the species in bulk solution and membrane phase are listed in Table S1 of the Supplementary Material. For the 1 M NaCl bulk electrolyte at neutral pH, which has a hydroxide ion concentration of 1.73 x 10^{-7} M, the concentration versus distance profiles in Figure 4a are nearly linear, with the slopes proportional to the current density. Figure 4b shows that the OH^- concentrations at the bipolar interface are nearly linearly dependent on the current density in the 1 M NaCl electrolyte, and that a maximum hydroxide ion concentration of 2.19 M is reached at a current density of 100 mA/cm^2. This indicates that even when producing very dilute base solutions, hydroxide ion concentrations inside the AEL can be substantially greater than 1 M, and that operating the system at a low current density can be used to minimize hydroxide concentrations in the AEL. For the 1 M NaOH bulk electrolyte solution, the OH^- concentrations range from 3.15 to 3.77 M, and are only weakly dependent on the current density, as shown in Figure 4b. The higher AEL hydroxide concentrations for the 1 M NaOH bulk electrolyte result from the fact that only hydroxide ions are available for balancing the Donnan potential inside the AEL. The Donnan potential, combined with a higher OH^- activity coefficient in the aqueous phase (γ_{aq}=0.58) compared to the membrane phase (γ_m=0.52), resulted in a 3.77 times greater OH^- concentration at the bipolar interface than in the bulk electrolyte. The weak dependence of the OH^- concentrations on the current density in Figure 4b indicate that operating the system at high current density will not significantly increase AEL hydroxide ion concentrations for bulk solutions containing a high ratio of OH^- to Cl^- concentrations.

For the 1 M NaCl bulk electrolyte, diffusion of chloride ions into the AEL was able to counter the Donnan potential. As shown in Figure 4b, chloride concentrations at the bipolar interface are 2.6 times greater than the bulk solution concentration at 0 mA/cm^2 and 1.7 times greater at 100 mA/cm^2. At the bipolar interface, the presence of 1 M Cl^- in the bulk solution reduced the hydroxide concentrations inside the AEL by 1.58 M at 100 mA/cm^2, 2.52 M at 50 mA/cm^2 and 3.48 M at 10 mA/cm^2. This indicates that maintaining a high concentration of anions in the bulk solution can substantially reduce hydroxide concentrations in the AEL.

Chloride ions in the bulk electrolyte also lead to more than a 3.5 times higher hydroxide ion concentration gradient inside the AEL. The concentration gradient will affect the contribution of diffusion to the overall transport of OH^- through the AEL. For the purpose of analysis, the concentration profiles in Figure 4a can be approximated as linear. For 100 mA/cm^2, the hydroxide ion concentration gradient for the 1 M NaCl electrolyte can be approximated as 219 mol/(L cm), and for the 1 M NaOH electrolyte, the approximate concentration gradient is 61.5 mol/(L cm). The contribution of diffusion to the steady state flux of OH^- can be calculated from:

$$diffusion\ flux = D\ \frac{dC}{dx} \quad (18)$$

Table 2
Bulk solution activity coefficients for the modeling results in Figure 3.

Species	1 M NaCl+0.1 M NaOH	1 M NaCl+0.1 M HCl
OH^-	0.551	0.513
H^+	0.925	0.993
Cl^-	0.598	0.598
Na^+	0.713	0.738

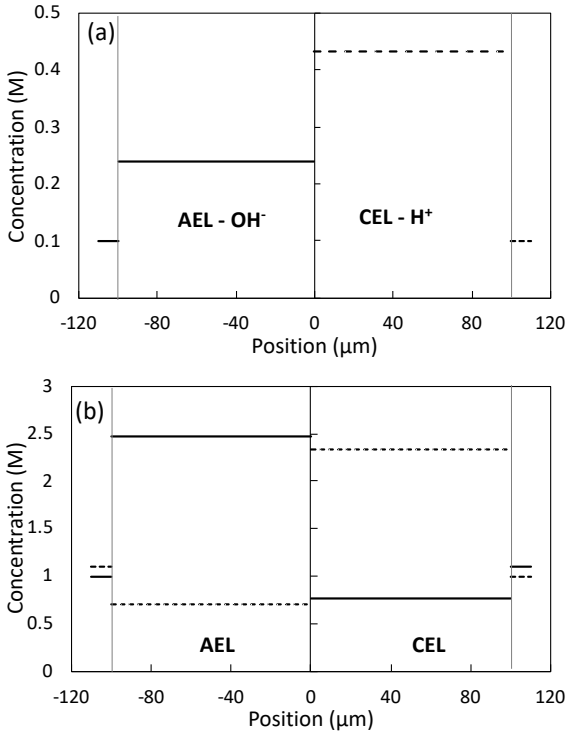

Fig. 3. Ion concentration profiles inside the AEL and CEL with no current applied for bulk solutions consisting of: 1 M NaCl + 0.1 M NaOH at x=-100 µm and 1 M NaCl + 0.1 M HCl at x=100 µm. a) concentration of OH^- in AEL (solid line) and H^+ in CEL (dashed line); (b) concentrations of Cl^- (solid line) and Na^+ (dashed line) CEL.

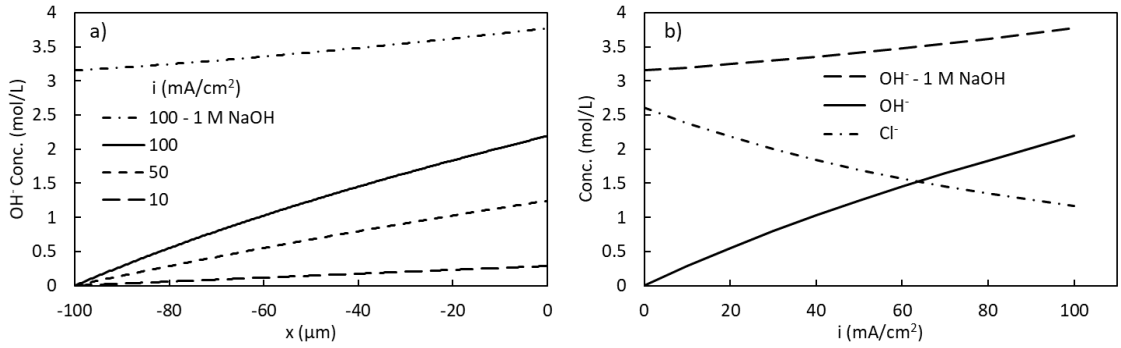

Fig. 4. a) Hydroxide ion concentrations in the AEL for a bulk solution of 1 M NaCl at current densities of 10, 50 and 100 mA/cm^2. Also shown are hydroxide concentrations for a bulk solution of 1 M NaOH at a current density of 100 mA/cm^2 (dot-dashed line). b) Hydroxide concentrations at the bipolar interface as a function of current density for bulk solutions of 1 M NaCl (solid line) and 1 M NaOH (dashed line). Also shown are Cl^- concentrations for a bulk solution of 1 M NaCl (dot-dashed line).

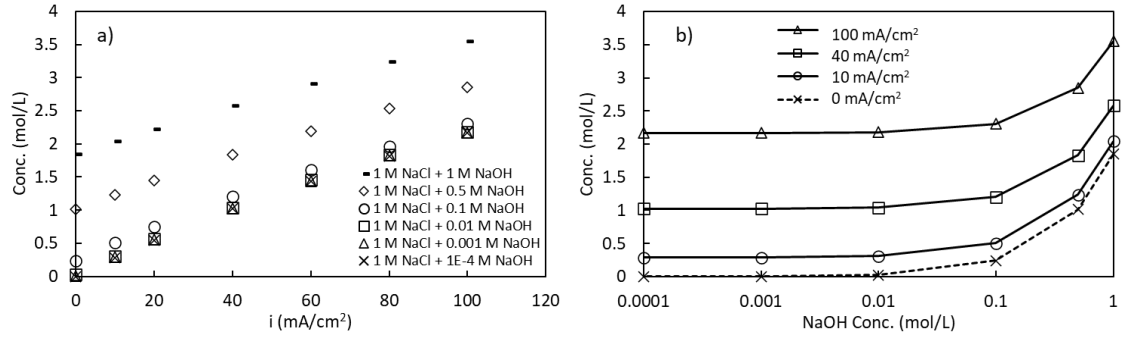

Fig. 5. a) Hydroxide concentrations at the bipolar interface as a function of current density for 1 M NaCl bulk electrolyte solutions with varying hydroxide concentrations. b) Hydroxide concentrations at the bipolar interface as a function of the NaOH concentration in 1 M NaCl bulk electrolyte solutions for current densities of 0, 10, 40 and 100 mA/cm^2.

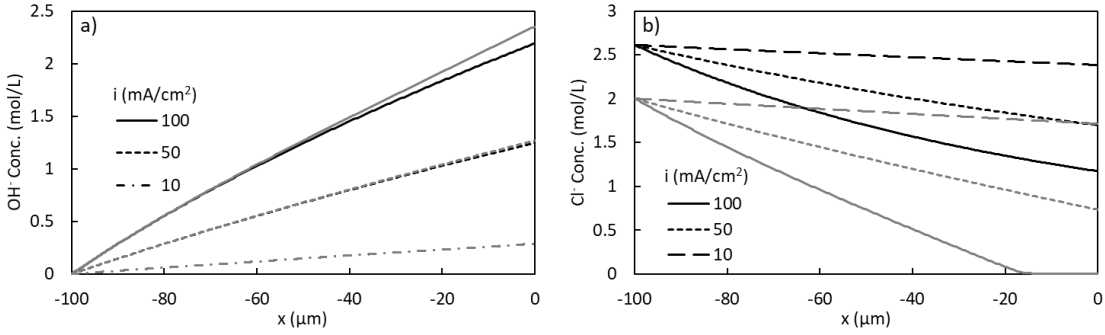

Fig. 6. a) Hydroxide concentrations in the AEL as a function of current density for 0.01 and 1 M NaCl bulk electrolyte solutions. Black lines represent 1 M NaOH and grey lines represent 0.01 M NaOH. b) Chloride concentrations in the AEL as a function of current density for 0.01 (grey lines) and 1 (black lines) M NaCl bulk electrolyte solutions.

and the total hydroxide flux can be calculated as:

$$total\ hydroxide\ flux = \frac{i}{96485\ C/mol} \tag{19}$$

where i is the current density. For the 1 M NaCl electrolyte at 100 mA/cm^2, the approximate diffusion flux is 7.6 x 10^{-7} mol/(cm^2 s) and the total hydroxide flux is 1.04 x 10^{-6} mol/(cm^2 s). Thus, the diffusive flux accounts for 73% of the total hydroxide flux for the 1 M NaCl electrolyte. For the 1 M NaOH electrolyte, the diffusive flux accounts for 20% and electromigration accounts for 80% of the total hydroxide flux at 100 mA/cm^2. At lower current densities, diffusion accounts for a smaller fraction of the hydroxide flux. At 50 mA/cm^2, diffusion accounts for 71% of the flux in 1 M NaCl and 14% of the flux in 1 M NaOH.

The effect of bulk solution NaOH concentrations on hydroxide concentrations at the bipolar interface are shown in Figure 5 for bulk solutions also containing 1 M NaCl. For all current densities, bulk solution hydroxide ion concentrations ≤ 0.1 M have little effect on the maximum hydroxide concentration in the AEL (which occurs at the bipolar interface). For a current density of 100 mA/cm^2, the maximum OH^- concentration in the AEL will be at least 2.2 M, regardless of the bulk solution hydroxide concentration. However, increasing the bulk solution hydroxide concentration above 0.1 M results in significant increases in the OH^- concentrations at the bipolar interface. These results indicate that attempting to minimize OH^- concentrations in the AEL by making dilute hydroxide solutions ≤ 0.1 M may be an effective strategy.

The effect of the bulk electrolyte concentration on AEL hydroxide concentrations are shown in Figure 6a for 0.01 and 1 M NaCl bulk electrolyte

solutions. For all three current densities, there was only a small effect of the NaCl concentration on hydroxide concentration profiles. Figure 6b shows that even a 0.01 M Cl^- concentration was able to counter the Donnan potential in the AEL, and thereby considerably reduce the hydroxide concentrations compared to a bulk solution without any Cl^- ions, as shown in Figure 4b. The 1 M NaCl bulk electrolyte resulted in significantly higher Cl^- concentrations in the AEL, as shown in Figure 6b. However, the higher negative charge in the AEL in the 1 M NaCl was countered by significantly higher Na^+ concentrations, as shown in Figure S1 of the Supporting Material.

3.3. Membrane thickness effects

The effects of membrane thickness on hydroxide concentrations in the AEL are shown in Figure 7a and b for a current density of 100 mA/cm^2 and a bulk solution consisting of 1 M NaCl plus 0.1 M or 0.5 M NaOH. Hydroxide concentrations in the AEL increased with membrane thickness, but the concentration increase was less than proportional to the increase in thickness. For example in Figure 7a, increasing the membrane thickness from 50 to 100 µm, increased OH^- concentrations by ~65%, and a factor of 5 increase in membrane thickness from 20 to 100 µm resulted in a factor of 3.1 increase in hydroxide concentrations. The effect of membrane thickness on hydroxide concentrations decreased with increasing bulk solution hydroxide concentration. Comparison of Figures 7a,b shows that the effect of membrane thickness on AEL hydroxide concentrations in the 0.5 M NaOH solution was approximately 50% less than that in the 0.1 M NaOH solution. Figure S2 in the Supplementary Materials shows the effect of membrane thickness for a 1 M NaOH solution. In this case, there is only ~15% greater concentrations in the 100 µm-thick membrane as compared to the 20 µm membrane. Thus, the effect of membrane thickness on AEL hydroxide concentrations decreases with increasing bulk solution hydroxide concentrations.

3.4. Ion exchange capacity effects

The effect of ion exchange capacity (IEC) on hydroxide ion concentrations in the AEL is shown in Figure 8a, for IEC values ranging from 0.5 to 2.0 eq/L for a bulk solution containing 0.1 M NaOH. Increasing ion exchange capacity leads to increasing hydroxide ion concentrations in the AEL, but the effect is small. A factor of 4 increase in the ion exchange capacity from 0.5 to 2.0 eq/L results in only a ~3% increase in hydroxide concentrations. However, the effect of ion exchange capacity increases with increasing bulk solution hydroxide ion concentrations. Figure 8b compares hydroxide concentrations as a function of ion exchange capacity for a solution with a bulk hydroxide concentration of 0.5 M. In this case, the factor of 4 increase in ion exchange capacity results in a 15 to 85% increase in AEL hydroxide concentrations. For a bulk solution with a 1 M hydroxide ion concentration, the factor of 4 increase in ion exchange capacity results in a 30 to 88% increase in AEL hydroxide concentrations, as shown in Figure S3 in the Supplementary Material. This trend results from an increasing fraction of the ion exchange capacity being compensated by OH^- versus Cl^- with increasing bulk solution hydroxide concentrations.

4. Conclusions

These modeling results show that the hydroxide ion concentrations in the AEL of bipolar membranes are significantly affected by the current density, bulk electrolyte concentration, bulk solution hydroxide concentration, AEL ion exchange capacity and AEL thickness. The hydroxide ion concentration profiles throughout the AEL are near linear over a wide range of operating conditions. For low bulk solution hydroxide concentrations (<0.1 M), hydroxide concentrations in the AEL are proportional to the current density, and are up to a factor of 20 or more times greater than the bulk solution concentration. For bulk solution hydroxide concentrations of 1 M, hydroxide concentrations in the AEL reach as high as 3.77 M at the bipolar interface. Bulk solution hydroxide ion concentrations have a significant effect on AEL concentrations only for concentrations exceeding 0.1 M. To prolong membrane life, AEL concentrations of hydroxide ions can be minimized by producing bulk solution hydroxide concentrations less than 0.1 M while operating the membrane at low current densities with high bulk electrolyte anion concentrations.

These suggestions for minimizing AEL hydroxide ion concentrations are antithetical to the goals of making concentrated acids and bases of high purity. For example, production of high purity NaOH that does not contain other anions, such as Cl^- or SO_4^{2-}, will require that the Donnan potential be compensated by only hydroxide anions. This will significantly increase AEL hydroxide concentrations. However, many applications do not require high purity or highly concentrated acids and bases. In water treatment applications, large volumes of low purity dilute acids and bases (i.e. ≤0.1 M) can achieve the same pH modulation effects as smaller volumes of more concentrated reagents. However, these applications would require onsite production to eliminate the high costs associated with transportation of dilute reagents.

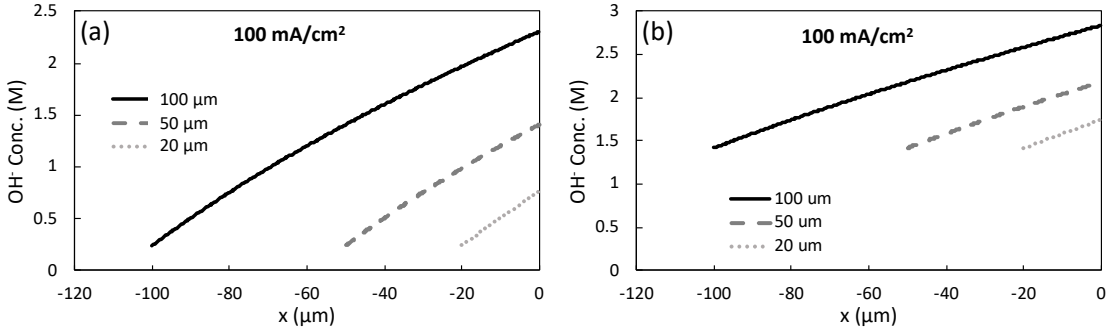

Fig. 7. a) Hydroxide concentrations for AEL thicknesses of 20, 50 and 100 µm for a bulk solution consisting of 1 M NaCl plus 0.1 M NaOH. b) a) Hydroxide concentrations for AEL thicknesses of 20, 50 and 100 µm for a bulk solution consisting of 0.5 M NaCl plus 0.5 M NaOH.

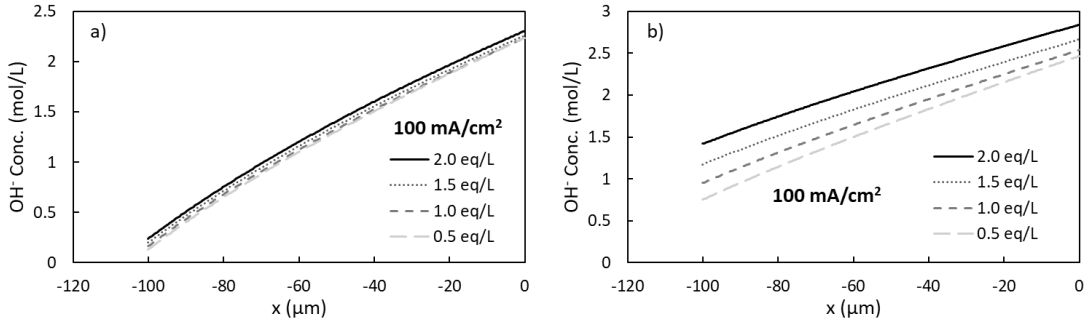

Fig. 8. Hydroxide concentrations in the AEL at 100 mA/cm^2 for a bulk solution consisting of (a) 1 M NaCl plus 0.1 M NaOH and (b) 0.5 M NaCl plus 0.5 M NaOH for a range in ion exchange capacities.

Acknowledgements

This research was supported by the National Science Foundation Chemical, Bioengineering, Environmental and Transport Systems (CBET) Division through Grant #1604857.

References

[1] M. Reig, C. Valderrama, O. Gibert, J.L. Cortina, Selectrodialysis and bipolar membrane electrodialysis combination for industrial process brines treatment: Monovalent-divalent ions separation and acid and base production, Desalination 399 (2016) 88–95. doi:10.1016/J.DESAL.2016.08.010.

[2] M. Badruzzaman, J. Oppenheimer, S. Adham, M. Kumar, Innovative beneficial reuse of reverse osmosis concentrate using bipolar membrane electrodialysis and electrochlorination processes, J. Membr. Sci. 326 (2009) 392–399. doi:10.1016/J.MEMSCI.2008.10.018.

[3] Y. Chen, J.R. Davis, C.H. Nguyen, J.C. Baygents, J. Farrell, Electrochemical ion-exchange regeneration and fluidized bed crystallization for zero-liquid-discharge water softening, Environ. Sci. Technol. 50 (2016). doi:10.1021/acs.est.5b05606.

[4] S. Mikhaylin, L. Patouillard, M. Margni, L. Bazinet, Milk protein production by a more environmentally sustainable process: bipolar membrane electrodialysis coupled with ultrafiltration, Green Chem. 20 (2018) 449–456. doi:10.1039/C7GC02154B.

[5] S. Pelletier, É. Serre, S. Mikhaylin, L. Bazinet, Optimization of cranberry juice deacidification by electrodialysis with bipolar membrane: Impact of pulsed electric field conditions, Sep. Purif. Technol. 186 (2017) 106–116. doi:10.1016/J.SEPPUR.2017.04.054

[6] A. Merkel, A.M. Ashrafi, J. Ečer, Bipolar membrane electrodialysis assisted pH correction of milk whey, J. Membr. Sci. 555 (2018) 185–196. doi:10.1016/J.MEMSCI.2018.03.035.

[7] X. Sun, H. Lu, J. Wang, Recovery of citric acid from fermented liquid by bipolar membrane electrodialysis, J. Clean. Prod. 143 (2017) 250–256. doi:10.1016/J.JCLEPRO.2016.12.118.

[8] P. Pinacci, M. Radaelli, Recovery of citric acid from fermentation broths by electrodialysis with bipolar membranes, Desalination. 148 (2002) 177–179. doi:10.1016/S0011-9164(02)00674-4.

[9] A.T.K. Tran, P. Mondal, J. Lin, B. Meesschaert, L. Pinoy, B. Van der Bruggen, Simultaneous regeneration of inorganic acid and base from a metal washing step wastewater by bipolar membrane electrodialysis after pretreatment by crystallization in a fluidized pellet reactor, J. Membr. Sci. 473 (2015) 118–127. doi:10.1016/J.MEMSCI.2014.09.006.

[10] J.R. Davis, Y. Chen, J.C. Baygents, J. Farrell, Production of acids and bases for ion exchange regeneration from dilute salt solutions using bipolar membrane electrodialysis, ACS Sustain. Chem. Eng. 3 (2015) 2337–2342. doi:10.1021/acssuschemeng.5b00654.

[11] R.J. Martinez, Y. Chen, D. Gervasio, J.C. Baygents, J. Farrell, Alkaline stability of novel aminated polyphenylene-based polymers in bipolar membranes, J. Membrane Sci. Res. 6 (2020) 218-225. doi: 10.22079/JMSR.2019.115517.1298.

[12] J. Farrell, R.J. Martínez, Understanding hydroxide reactions with guanidinium-based anion exchange polymers under conditions relevant to bipolar membrane electrodialysis, J. Comput. Theor. Chem. 1155 (2019) 75-81. doi:10.1016/j.comptc.2019.03.020

[13] H. Strathmann, Ion-exchange Membrane Separation Processes, Vol. 9, Elsevier, Amsterdam, 2004.

[14] H. Strathmann, J.J. Krol, H.J. Rapp, G. Eigenberger, Limiting current density and water dissociation in bipolar membranes, J. Mem. Sci. 125 (1997) 123–142. doi:10.1016/S0376-7388(96)00185-8

[15] F.G. Donnan, The theory of membrane equilibria, Chem. Rev. 1 (1924) 73–90. doi:10.1021/cr60001a003.

[16] C.R. Visser, Electrodialytic recovery of acids and bases, University of Groningen, 2017. https://www.rug.nl/research/portal/files/14524647/thesis.pdf (accessed December 21, 2020).

[17] M.B. McDonald, M.S. Freund, Graphene oxide as a water dissociation catalyst in the bipolar membrane interfacial layer, ACS Appl. Mater. Interfaces 6 (2014) 13790–13797. doi:10.1021/am503242

[18] F.G. Wilhelm, I. Pünt, N.F.A. van der Vegt, M. Wessling, H. Strathmann, Optimisation strategies for the preparation of bipolar membranes with reduced salt ion leakage in acid−base electrodialysis. J. Membr. Sci. (182) 2001, 13−28. doi:10.1016/S0376-7388(00)00519-6

[19] R.F. Probstein, Physicochemical Hydrodynamics : An Introduction, John Wiley & Sons, New York, 2005.

[20] K.E. Brenan, S.L. Campbell, L.R. Petzold, Numerical solution of initial-value problems in differential-algebraic equations, Vol. 14, Society for Industrial and Applied Mathematics, Philadelphia, 1996.

[21] L.F. Shampine, M.W. Reichelt, The MATLAB ODE suite, J. Sci. Comput. 18 (1997) 1–22. doi:10.1137/S1064827594276424.

[22] D.L. Parkhurst, C.A.J. Appelo, Description of input and examples for PHREEQC version 3—a computer program for speciation, batch-reaction, one-dimensional transport, and inverse geochemical calculations. U.S. Geological Survey Techniques and Methods, 2013. available only at https://pubs.usgs.gov/tm/06/a43/

[23] J. Kamcev, D.R. Paul, B.D. Freeman, Ion activity coefficients in ion exchange polymers: applicability of Manning's counterion condensation theory, Macromolecules 48 (2015) 8011−8024. doi:10.1021/acs.macromol.5b01654